ELSEVIER

International Journal of Pharmaceutics 238 (2002) 215–228

international journal of pharmaceutics

www.elsevier.com/locate/ijpharm

Polymorphism of the CNS active drug Org 13011: the application of high temperature analysis to detect new polymorphs

P. van Hoof [a,*], R. Lammers [b], R. v. Puijenbroek [b], M. v/d Schans [a], P. Carlier [c], E. Kellenbach [c]

[a] *Analytical Chemistry for Development, Organon, P.O. Box 20, 5340 BH Oss, The Netherlands*
[b] *Chemicals Research Arnhem, AkzoNobel, P.O. Box 9300, 6800 SB Arnhem, The Netherlands*
[c] *Process Chemistry, Organon-Riom, 63203 Riom, France*

Received 18 September 2001; received in revised form 15 February 2002; accepted 18 February 2002

Abstract

The polymorphism of the CNS active compound Org 13011 was studied using different crystallisation methods (i.e. different solvents and cooling rates). The samples were analysed by Raman, solid state NMR, X-ray powder diffraction (XRPD) and thermal analysis. This led to the characterisation of two crystalline forms A and B. Further high temperature analysis using Raman, XRPD, solid state NMR and DSC revealed another two (high temperature) crystalline forms C and D. The transitions to the high temperature crystalline forms occur at temperatures of about 60 °C. This study shows that the application of high temperature experiments is useful and can lead to the discovery of new crystalline forms. © 2002 Published by Elsevier Science B.V.

Keywords: Polymorphism; X-ray powder diffraction; Solid state NMR; CNS active drug; Crystallisation; High temperature analysis

1. Introduction

Org 13011 or 1-[4-[4-[4-(trifluoromethyl)-2-pyridinyl]-1-piperazinyl] butyl]-2-pyrrolidinone (E)-2-butenedioate (1:1) Fig. 1, is a central nervous system active compound. To explore the different crystalline forms a comprehensive polymorphism study was performed.

Polymorphism, that is the existence of a compound in more than one crystalline form, is a well-known phenomenon (Mitscherlich, 1822; Groth, 1877; Ostwald, 1897; Chamot and Mason, 1938; Kofler et al., 1954; Bernstein, 1999). One of the first written statements of polymorphism is that of Mitscherlich (Mitscherlich, 1822). He states: ‘‘It is a certain consequence that one and the same substance, composed of the same elements, combined in the same properties, can exhibit two different forms, provided that the particular circumstances exert an influence on the

* Corresponding author. Tel.: +31-412-663-602; fax: +31-412-663-513.
E-mail address: peter.vanhoof@organon.com (P. van Hoof).

0378-5173/02/$ - see front matter © 2002 Published by Elsevier Science B.V.
PII: S0378-5173(02)00073-X

act of crystallisation". Although the issue of polymorphism is very old and also some of the examples of polymorphism of pharmaceutical compounds are old, e.g. Chloramphenicol palmitate (Aguiar et al., 1967; De Villiers et al., 1991, 1993; Mitra et al., 1993), Novobiocin (Mullins and Macek, 1959) and Aspirin (Tawashi, 1969), it is only more recently, that it has become an issue in the development of drugs. A recent example is the HIV protease inhibitor Norvir (ritonavir) of Abbot (The Pharmaceutical Journal, 1998), which, after 2 years of production, crystallised in a new form that does not dissolve. It is also known that the chemical and physical stability and the bioavailability of the drug product and drug substance are related to the crystalline forms.

The analysis of different crystalline forms has been practised for many years (Haleblian and McCrone, 1969; Haleblian, 1975; Reffner and Ferrillo, 1988; Threfall, 1995; Kuhnert-Brandstatter and Sollinger, 1990a,b; Giron, 1995; Brittain, 1997). Techniques like microscopy, spectroscopy (infrared, Raman and solid state NMR), thermal analysis (DSC, DTA and TG), X-ray diffraction and hot-stage analysis (e.g. optical and infrared microscopic) are well established for both characterisation and quantification of different crystalline forms (Kuhnert-Brandstatter and Sollinger, 1990a,b; Giron, 1995; Brittain, 1997). It is generally accepted that complementary analytical techniques should be used in conjunction with each other to be able to properly characterise all different crystalline forms. For quantification of different crystalline forms in a production environment usually a cost/benefit analysis determines the technique of choice.

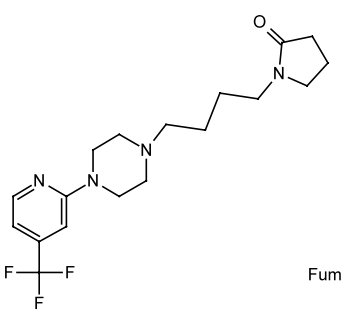

Fig. 1. The CNS active drug Org 13011.

In the case of Org 13011 a series of crystallisation experiments were performed in order to explore the effects of solvent and crystallisation temperature. The samples from these experiments were examined using Raman spectroscopy (Raman), solid state nuclear magnetic resonance spectroscopy (SS-NMR), thermal analysis (DSC and TG/DTA) and X-ray powder diffraction (XRPD). High temperature analysis by XRPD and SS-NMR revealed the existence of new high temperature phases.

2. Materials and methods

Each crystallisation experiment consisted of dissolving Org 13011 at the reflux temperature of the solvent of choice and crystallisation of the compound by slowly cooling to room temperature. Solvent mediated conversion experiments were performed to determine the most stable crystalline form. In such experiments, a slurry of a mixture of crystalline forms and solvent is stirred for a period of time at a certain temperature. Samples were taken as a function of time. The conditions for the different experiments are listed in Tables 1 and 2.

2.1. Raman spectroscopy

The spectra were recorded using a Bruker RFS 100/S spectrometer, equipped with a 1.064 μm Nd:YAG laser. For each sample 128 scans were collected, with a resolution of 2 cm^{-1}. Temperature experiments were performed using a Bruker heating stage with a Eurotherm 808 controller.

2.2. Solid state NMR

The 100.6 MHz solid-state ^{13}C CP-MAS NMR experiments were performed on a Bruker DRX400 NMR spectrometer. The 90° pulse was 4.5 μs and the cross polarization time 2.5 ms. Approximately 90 mg of the sample was weighed into a 4 mm rotor. The rotor speed was 8.0 kHz. The relaxation delay was 6.5 s. Some 4000 FIDs were accumulated before Fourier transformation.

Table 1
Conditions for the different crystallization experiments

Sample code	ss-NMR[a] (form)	DSC		Remarks
		T_{onset} (°C)	ΔH (mJ/mg)	
Batch I	A	62	11	Crystallised from ethanol (96°)
		136.8	96	
Batch II	A (75%)	66	8.6	Crystallised from ethanol (96°)
	B (25%)	138.4	94	
Batch III	A (10%)	57.3	1	Crystallised from ethanol (96°)
	B (90%)	138.8	95	
Batch IV	A	57.5	13	Crystallised from ethanol (96°)
		140.1	100	
Batch V	A	59	13	Crystallised from ethanol (96°)
		140.7	99	
Batch VI	A (80%)	61	11	Crystallised from ethanol (96°)
	B (20%)	141.1	101	
Batch VII	A (60%)	58	12	Crystallised from acetone
	B (40%)	141.2	102	
Batch VIII	A (10%)	57	3	Crystallised from ethyl acetate
	B (90%)	139.7	96	
Batch IX	A	60	13	Crystallised from acetonitril
		140.5	101	
Batch X	A	60.6	13	Crystallised from water
		141.2	101	
Batch XI	A (66%)	64	10	–
	B (34%)	116	0.3	
		140.1	96	
Batch XII	A	–	–	Sample used for high temperature experiments
Batch XIII	A (5%)	–	–	Sample used for high temperature experiments
	B (95%)			

[a] Percentages were calculated using semi-quantitative analysis by integrating peak surfaces, with an estimated error of 5%.

The measurements at elevated temperatures were performed on a Bruker MSL200 which operates at 50.3 MHz for ^{13}C. The following experimental conditions were used: a rotor speed of 5100 Hz, 2000–9000 FIDs, 2.5 ms CP-time, a ^{13}C $1/2\pi$ pulse of 3.9 μs, an acquisition time of 65 ms with a relaxation delay of 6.5 s and as a reference adamantane ($CH_2 = 38.56$ ppm from TMS = 0 ppm) was used. About 80 mg of samples was weighed into a 4 mm ZrO_2 spinner. To enhance the resolution the FIDs were multiplied with a Gaussian apodization function with LB = −10 Hz and GB = 0.1. The samples were measured at RT, at $T = 90$ °C (heating rate 1 °C/min) and after cooling to RT (cooling rate 1 °C/min) again. Also some semi-quantitative measurements were performed by integrating the different signals relative to each other. The estimated error is 5%.

2.3. Thermal analysis

The DSC curves were recorded using a Seiko DSC 120 instrument, in closed aluminium pans with a volume of 5 μl in combination and with a nitrogen flow of 50 ml/min. The heating rate was 5 °C/min. The TG and DTA curves were recorded simultaneously using a Seiko TG/DTA 220 instrument. Open aluminium pans were used in combination with a nitrogen flow of 100 ml/min. The heating rate was 5 °C/min. A series of samples were measured using a TA Instruments TA2920 in the standard mode. Using this set-up it was also possible to collect data during cooling, whereas with the set-up described above this was not possible. The heating (and cooling) rate was 10 °C/min. A helium flow rate of 25 ml/min was used as a purge gas over the cell.

Table 2
Details of the different crystallization experiments

Sample	Form	Stirring experiment in Ethanol (100%)
Batch XIVa	A (80%)	Batch VI used for stirring experiment at RF
	B (20%)	
Batch XIVb	A	Start of RF
Batch XIVc	A	Stirred at RF for 7 h
Batch XIVd	A	Stirred at RF for 24 h
Batch XVa	A (75%)	Start of stirring of suspension of batch B at −15 °C in ethanol
	B (25%)	
Batch XVb	A (90%)	Stirred at −15 °C for 1 h
	B (10%)	
Batch XVc	A	Stirred at −15 °C for 2 h
Batch XVd	A	Stirred at −15 °C for 3 h
Batch XVe	A	Stirred at −15 °C for 7 h

RF = 78 °C

2.4. X-ray powder diffraction (XRPD)

The XRPD were recorded on a Siemens D5000 θ–θ reflection diffractometer with Cu–K_α radiation and HTK oven for the high temperature experiments. Generator settings were 40 kV and 50 mA. The slits used: divergence and receiving slits V20 and the detector slit 0.2 mm; nickel filter. The measuring conditions: $2\theta = 5$–$35°$, step size 0.02°, time per step 5 s. The samples were measured at RT, 30, 40–100 °C, and after cooling to RT (delay 1 h). The measurements were carried out under a nitrogen flow.

3. Results and discussion

3.1. Crystallisation and slurry experiments

Thirteen different batches of Org 13011 were prepared by crystallisation from five different solvents employing different crystallisation methods. The samples were analysed using several analytical techniques to determine the polymorphic composition. These experiments, including the results from solid state NMR and DSC, have been summarised in Table 1. The results clearly show the existence of two crystalline forms, which will be described into more detail below.

It can be seen that crystallising from acetonitrile, water and ethanol lead to pure form A, however crystallisation from ethanol also leads to mixtures of crystalline forms A and B. This shows that repeating the same crystallisation in ethanol

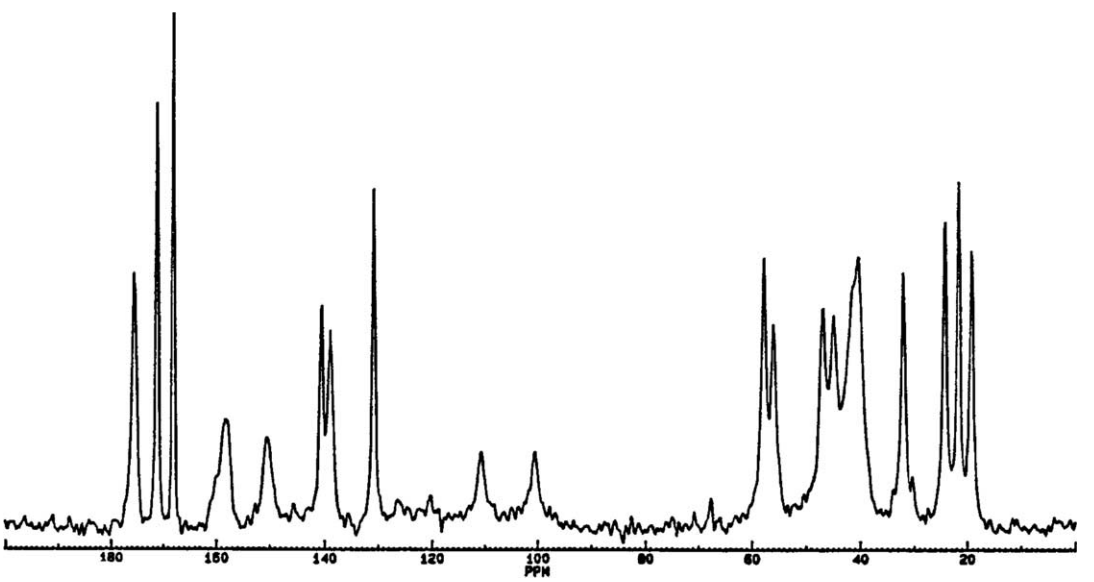

Fig. 2. SS-NMR spectrum of form A (XIVd) at ambient temperature.

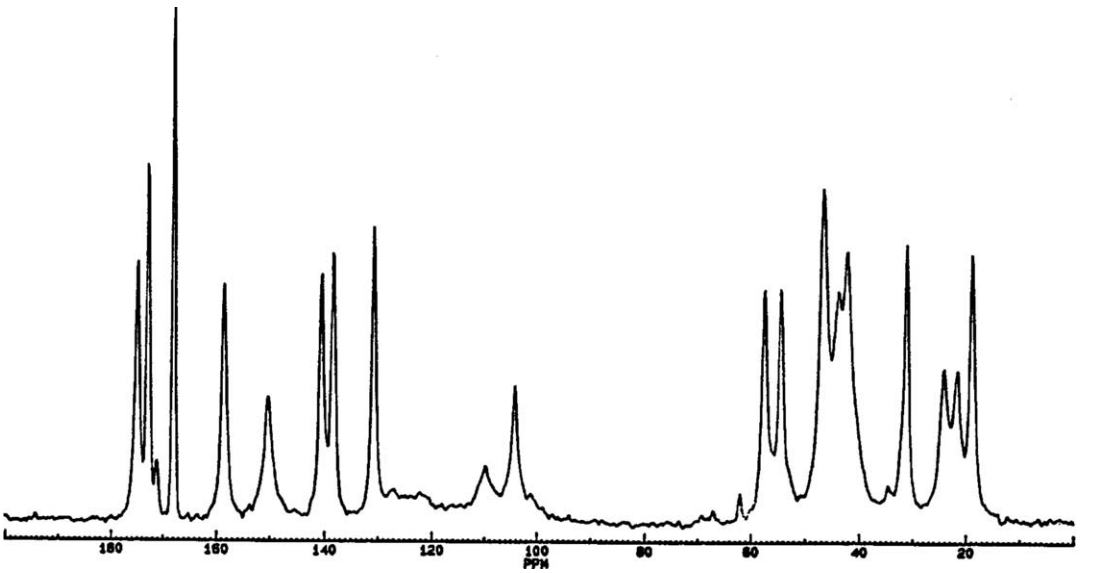

Fig. 3. SS-NMR of sample form B (VIII) at ambient temperature.

can lead to different mixtures of forms A and B. We do not know whether repeating the crystallisation from other solvents, e.g. acetone, ethyl acetate, acetonitril and water, also lead to different polymorphic compositions. Samples containing pure crystalline form B have never been obtained.

To determine the physical stability of both forms A and B, nine solvent mediated conversion experiments at −15 and at 78 °C were performed. Table 2 lists the results of these experiments, which show that at both temperatures a conversion from crystalline form B to crystalline form A occurs. The transition time varies from less than 1 h for slurry experiments at 78 °C to 2 h at −15 °C. These solution mediated transitions show that form A has the lowest solubility (and thus a lower Gibbs free energy) in this temperature range.

3.2. Low temperature forms

All analysis have been performed on the isolated solid state samples. The solid state NMR spectra of different batches clearly show that two crystalline forms exist. Figs. 2 and 3 show the solid state NMR spectra of a sample containing 100% form A and 90% form B (and 10% form A),

Table 3
Characteristic signals of the four polymorphs of Org 13011 using solid state NMR (SS-NMR), X-ray powder diffraction (XRPD) and Raman spectroscopy (Raman)

Technique	Form A	Form B	Form C	Form D
SS-NMR	32.1	31.3	32.0	31.9
(ppm)	171.1	172.8	172.0	172.8
	175.5	175.0	174.0	173.7
XRPD (2θ)	–	–	–	4.0
	4.16	4.26	3.96	4.18
	–	–	–	12.12
	–	16.26	16.01	16.04
	16.84	16.89	16.76	–
	–	17.16	18.30	18.76
	19.58	21.31	20.01	19.58
	–	–	–	21.07
	–	23.18	–	22.75
	24.23	23.88	24.59	24.16
	–	25.85	–	25.33
Raman	3081	3087	3081	3084
(cm^{-1})	3067	3058	3061	3057
	3025	3012	3029	3012
	1726	1719	1723	1719
	1665	1664	1660	1661
	986	982	986	981
	118	155	107	154

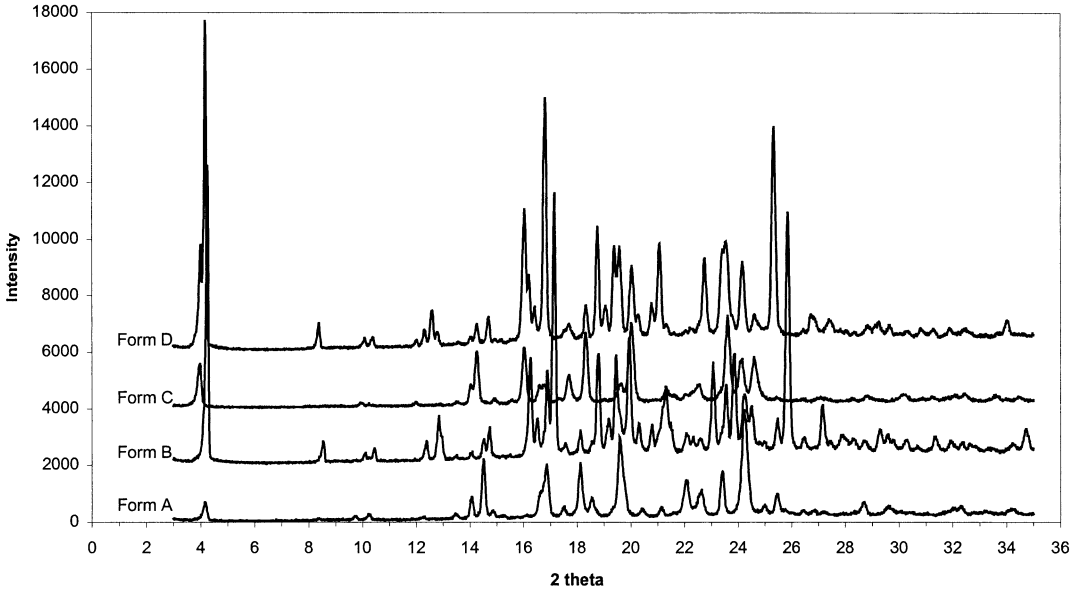

Fig. 4. Diffraction patterns of form A (lower trace), form B, form C and form D (upper trace).

respectively. The two forms have distinct signals, especially around 31, 171 and 174 ppm, see Table 3. The chemical shifts are similar to that of the ^{13}C NMR spectra from solution and the spectra of both forms clearly show only one signal per carbon atom. The latter indicates that the asymmetric crystal unit of both forms A and B consists of one molecule only. Those signals were used for the semi-quantitative analysis of forms A and B.

The XRPD patterns of forms A and B have been recorded (Fig. 4), and also show distinct differences. Table 3 lists the 2θs where the main differences in the diffraction patterns of the two polymorphs can be found.

Finally, Raman spectra have been recorded of both polymorphs A and B. Different signals from different polymorphs can also be found in these spectra, see Figs. 5 and 6, and Table 3. Hence, the analysis using SS-NMR, XRPD and Raman spectroscopy clearly proves the existence of two polymorphs.

Although the results from IR, Raman, SS-NMR and XRPD are straightforward, the results from DSC seemed contradictory. Fig. 7 shows the DSC curve of batch XII which is exclusively form A. This curve features a small endothermic peak at about 60 °C, and a melting peak at 141.6 °C. The endothermic peak at 60 °C suggests a enantiotropic relation (Giron, 1995; Burger and Ramberger, 1979; Yu, 1995) between form A and another crystalline form. Two crystalline forms show an enantiotropic relation if the free energy curves of the separate forms cross at some point below their melting temperatures. This indicates that the relative stability of the two forms change at the crossing point of the free energy curves. However, the possible high temperature crystalline form observed in the DSC is not form B, because it was showed that form B transforms to A and not otherwise.

Fig. 8 shows the DSC curve of batch VIII, containing 90% form B (and 10% form A). This curve also shows a small endothermic peak (at about 57 °C) and a melting peak at 139.7 °C. This endothermic peak again points towards an enantiotropic relation with an other crystalline form. Note that the TG curves did not show any weight loss before the melting of the polymorphs. Therefore, we do not expect solvates or degradation to play a role of importance. These DSC measurements give rise to several questions:

1. Are the endothermic peaks in the DSC curves at about 57 and 60 °C due to transitions to new crystalline forms?
2. Why is the small endothermic peak in the DSC curves so broad?

The first question will be addressed using high temperature analysis (Raman, XRPD and SS-NMR), whereas the latter is addressed using DSC with repeated runs and controlled cooling runs.

3.3. High temperature analysis

Experiments at elevated temperatures were performed for both polymorphs A and B, always on the isolated solid state samples, using SS-NMR, XRPD and Raman spectroscopy. Figs. 9 and 10 show the SS-NMR spectra at 90 °C of the two forms A and B. The X-ray diffraction patterns at elevated temperatures are shown in Figs. 4, 11 and 12 and the Raman spectra in Figs. 5 and 6. All three techniques clearly show that the spectra and diffractograms change when the samples are heated to above 70 °C. Table 3 lists the positions of the distinct signals of these spectra and diffractograms. It can also clearly be seen that the high temperature spectra and diffractograms are not identical to each other and also not identical to the spectra and diffractograms of neither form A nor B. These high temperature polymorphs are from now on called forms C and D. Also in all three techniques the transition from A to C and from B to D occurs fast (within a few minutes) and is reversible. Upon cooling, the polymorphs C and D transformed back to A and B, respectively.

A high temperature XRPD scan of form A showed a broad phase transition from 65 to

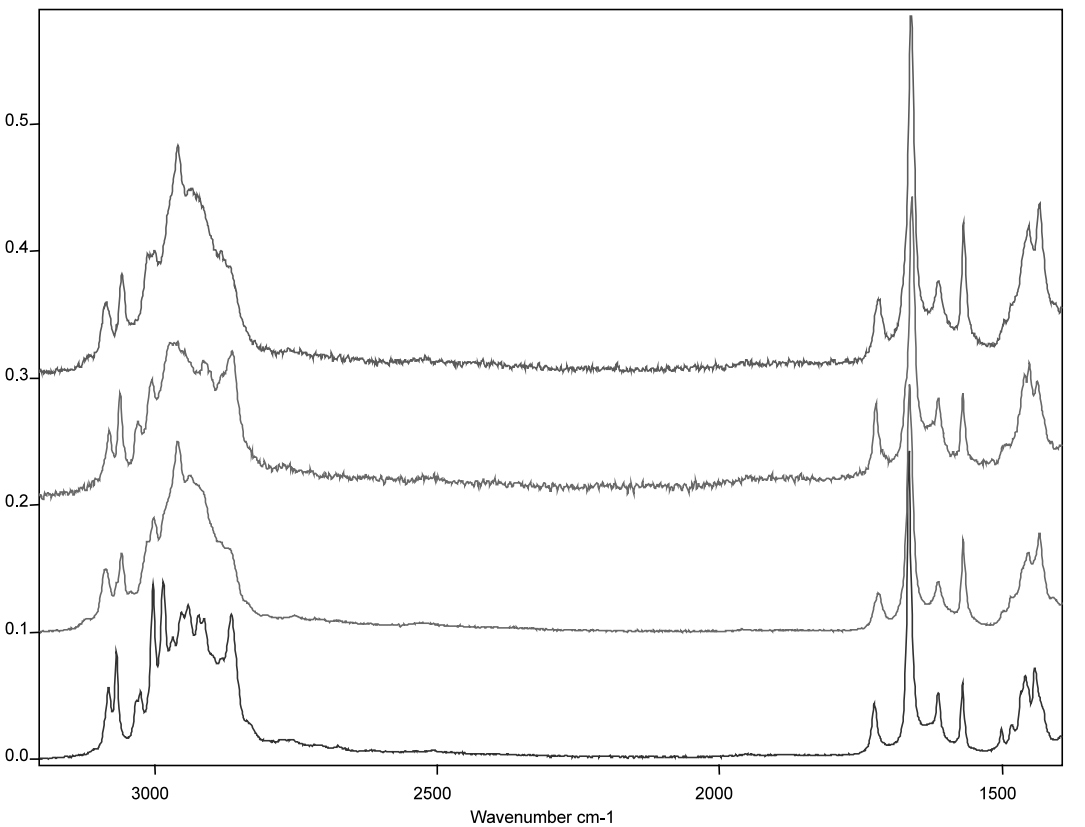

Fig. 5. Raman spectra (spectral region 3200–1400 cm^{-1}) of polymorphs A (lower trace), B, C and D (upper trace).

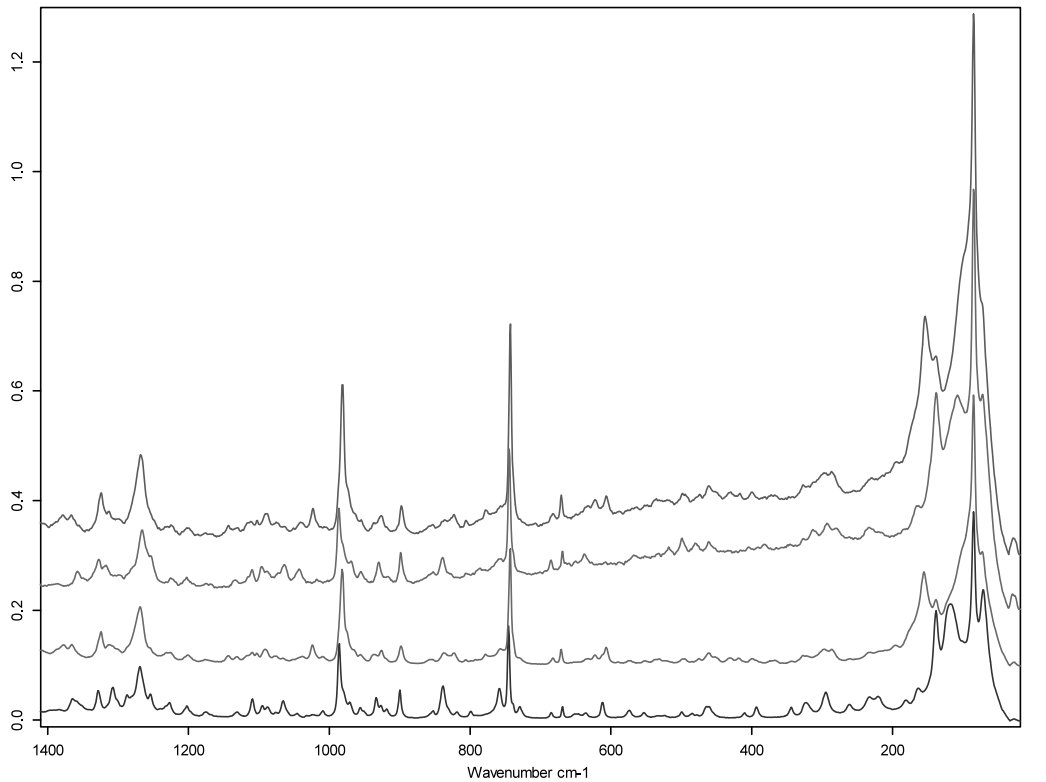

Fig. 6. Raman spectra (spectral region 1400–80 cm^{-1}) of polymorphs A (upper trace), B, C and D (upper trace).

100 °C (Fig. 11). After cooling to room temperature the pattern of form A was observed again. The phase transition from A to C is almost completely reversible because (only a few, or weak) reflections of form C could be observed in the pattern from the temperature cycled material. In a second high temperature scan of the same sample the phase transition from A to C was observed in the temperature range from 50 to 70 °C. The transitions observed in the two high temperature measurements are in agreement with those in the DSC experiments.

A high temperature XRPD scan of 90% form B (batch VIII) showed a phase transition between 60 and 70 °C (Fig. 12). Close examination of the high temperature XRPDs show that it is difficult to distinghuish between the phase transition and the shift of the peaks due to anisotropic expansion (note: the sample is heated!). However, it is clear that two new peaks appear at 2θ of 4.0 and 12.12 at high temperature and the peak at a 2θ of 16.89 disappear at high temperature (see Table 3). Moreover, the DSC patterns (Figs. 13 and 14) clearly show a endothermic effect just above 50 °C. We believe that these two observations lead to the conclusion that there exists a high temperature form D, which is distinct from low temperature form B.

Because batch VIII contained a small amount of form A ($\approx 10\%$) the high temperature phase of batch VIII also contained a small amount of form C. After cooling to room temperature the pattern was identical to the pattern of the starting batch VIII, leading to the conclusion that the phase transition of form B–D is reversible. The second high temperature XRPD scan of batch VIII is identical to the first high temperature scan which is in line with the second run of DSC. The thermal effect observed with DSC that was attributed to a relaxation process was not observed with high temperature XRPD.

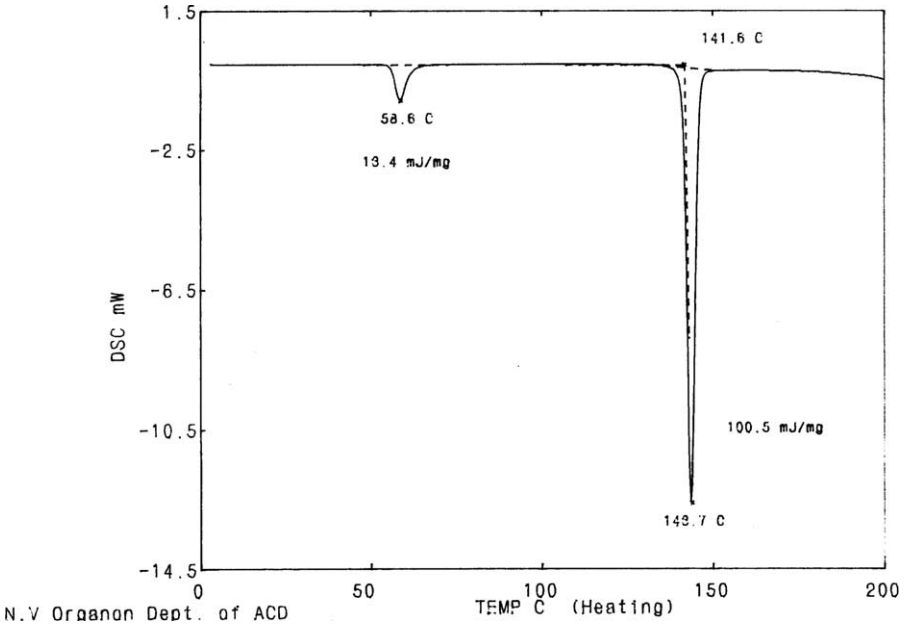

Fig. 7. DSC curve (heating rate 5 °C/min) of form A (batch XII).

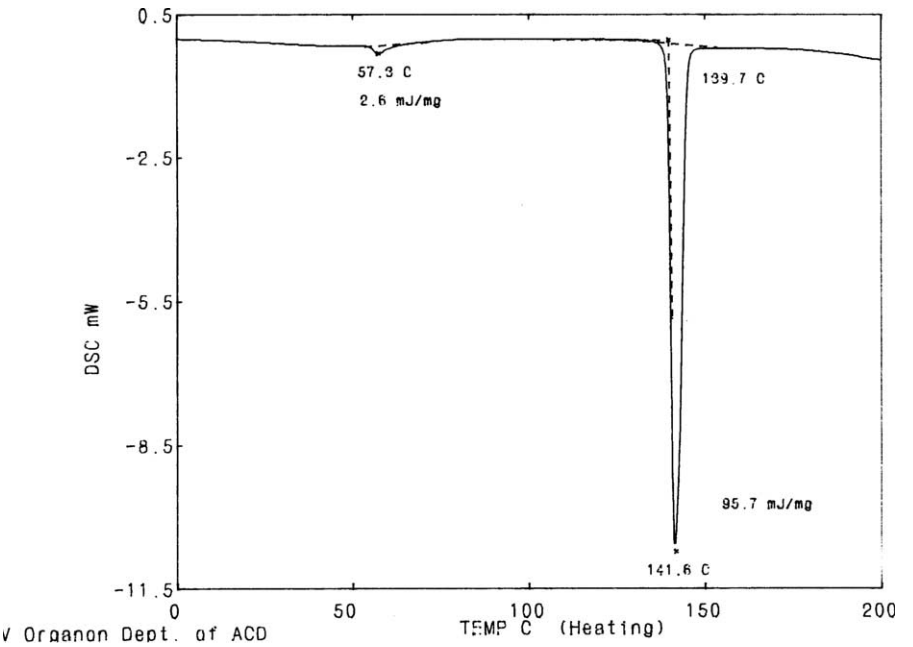

Fig. 8. DSC curve (heating rate 5 °C/min) of form B (batch VIII).

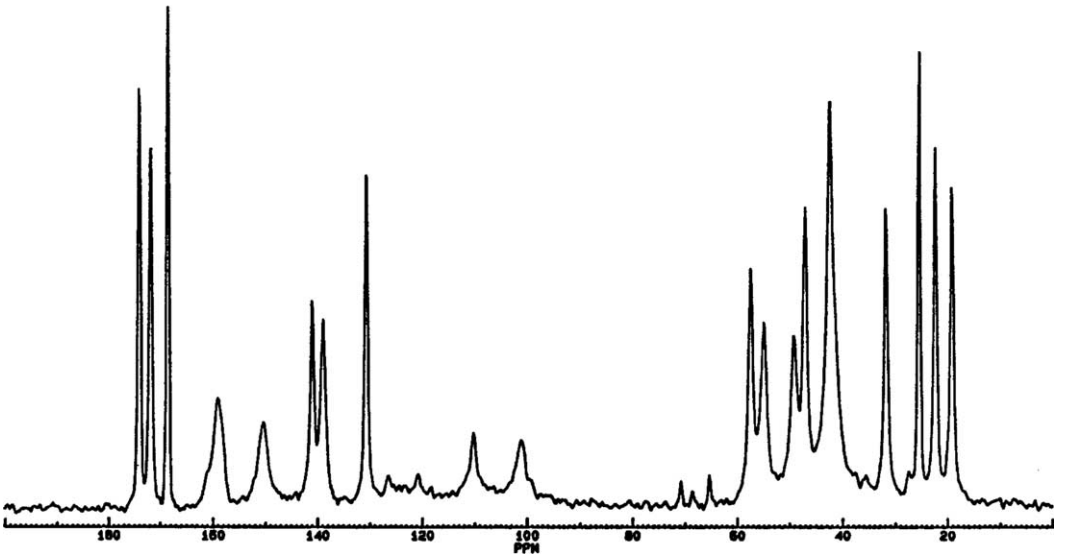

Fig. 9. SS-NMR spectrum of form C (batch XIVd at 90 °C).

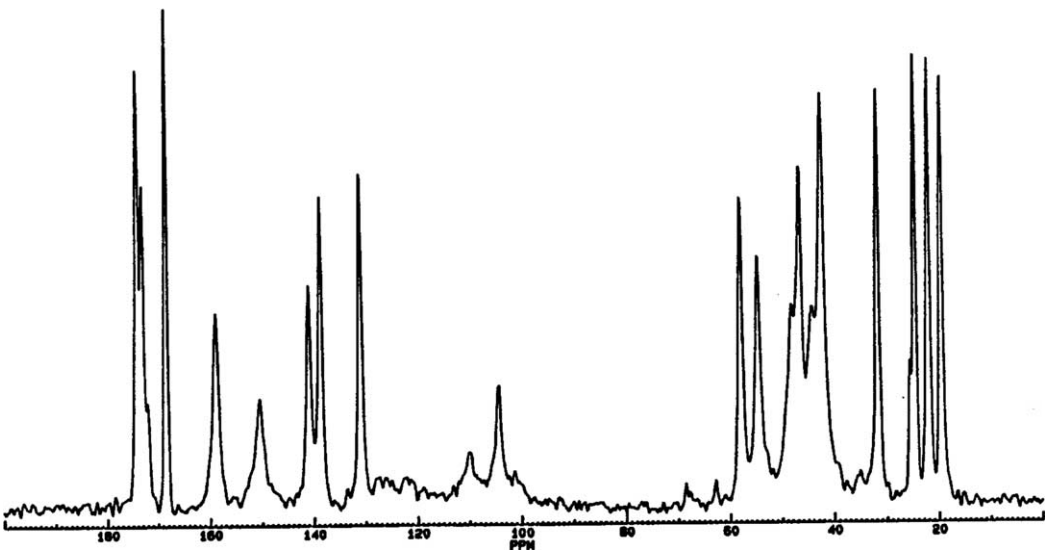

Fig. 10. SS-NMR spectrum of form D (batch VIII at 90 °C).

Figs. 13 and 14 (DSC) show that during the first heating run the two transitions were rather broad and the endothermic peak of form B seemed to exist of two superimposed thermal events. The exothermic peaks that were found upon cooling support the enantiotropic relation between the new crystalline forms and forms A and B. The second run showed two rather sharp endothermic peaks at approximately the same temperature. The difference of the shapes of the endothermic peaks of the first and second scan was probably due to differences in disorder in the crystalline state. Annealing a sample of form B at 50 °C, that is below the transition temperature of

60 °C, resulted in a crystalline state without disorder and thus a sharp endothermic peak is observed, see Fig. 14.

The relative stability's of forms A–D can be deduced from these experiments and have been indicated by Fig. 15. Polymorphs A and B are formed directly upon crystallisation, whereas polymorphs C and D can only be formed upon heating forms A and B. Form C is obtained by heating form A, and form D is obtained by

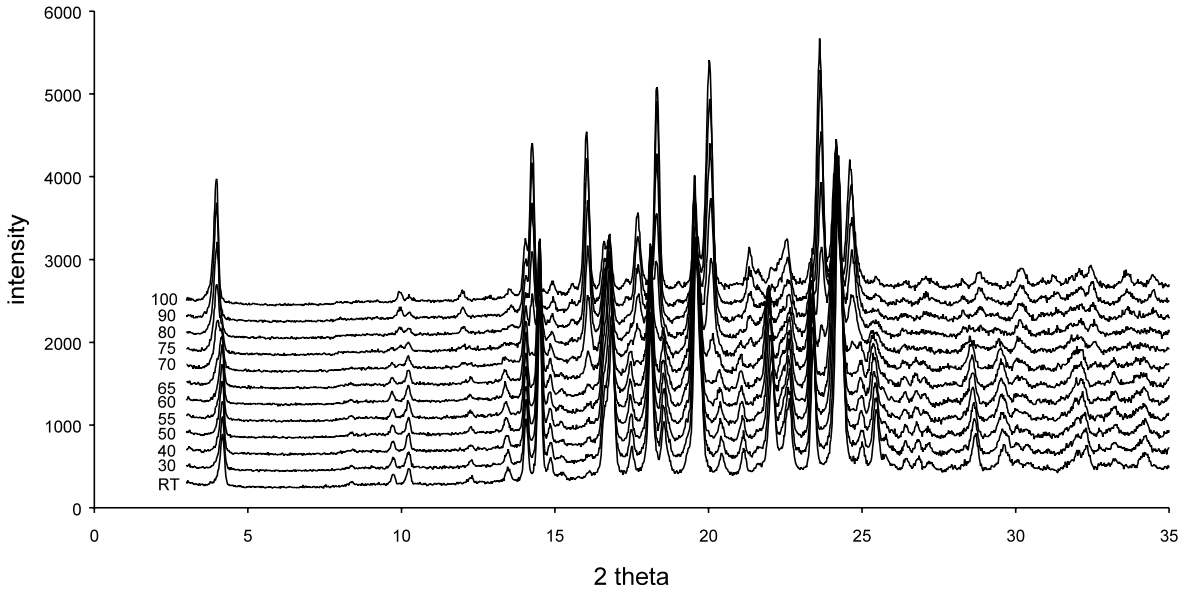

Fig. 11. XRPD high temperature scan of form A.A phase transition is observed between 65 and 100 °C.

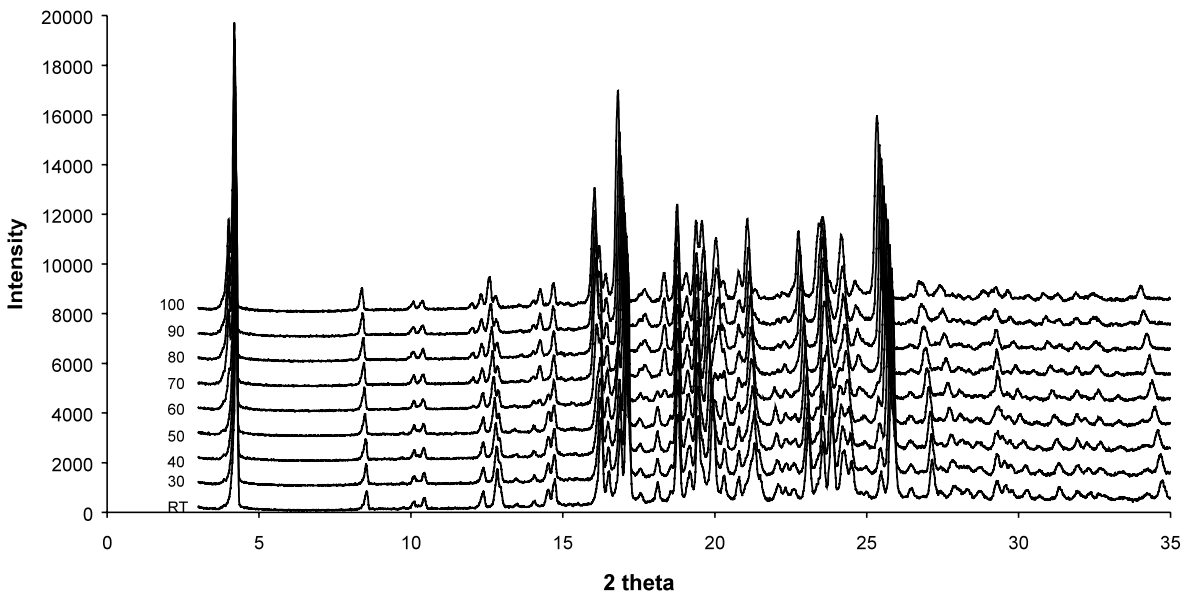

Fig. 12. XRPD high temperature scan of form B. A phase transition is observed between 60 and 70 °C.

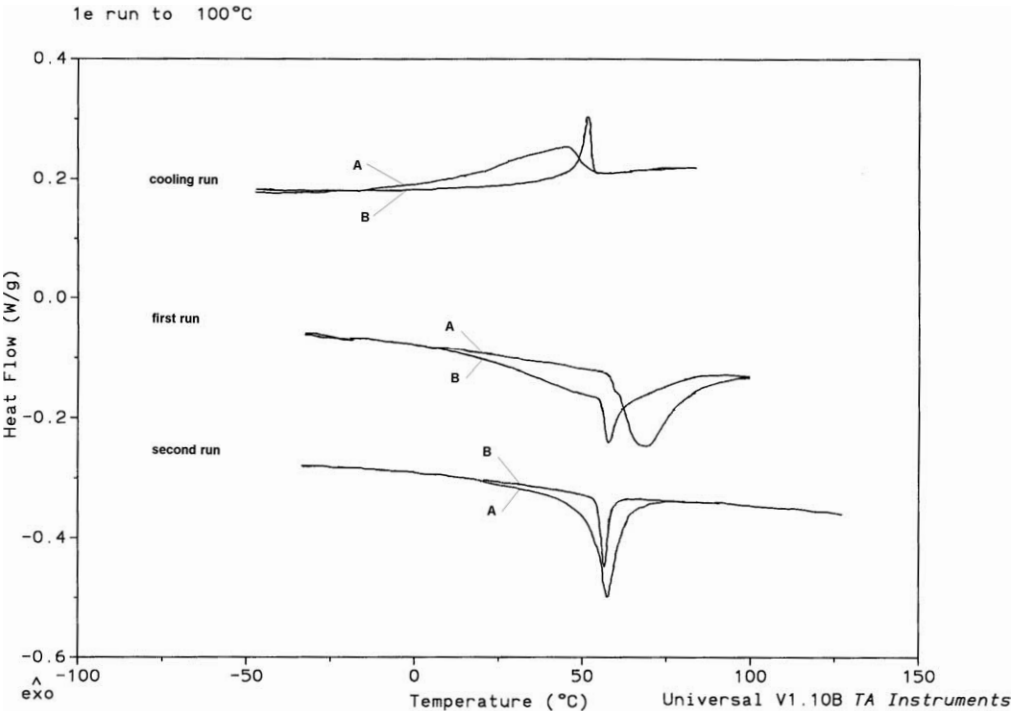

Fig. 13. DSC of forms A and B using a heating and cooling rate of 10 °C/min.

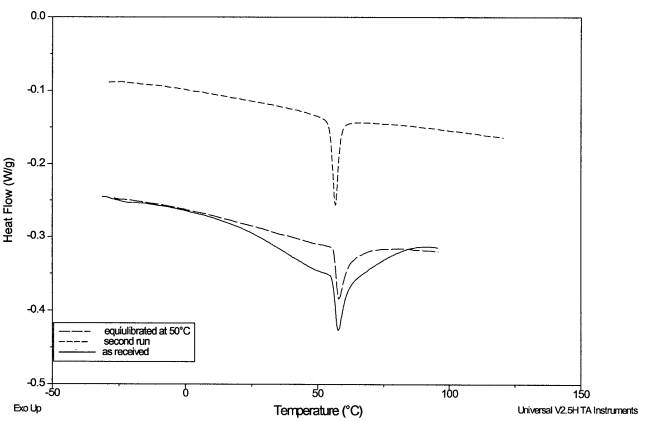

Fig. 14. DSC curves (heating and cooling rate 10 °C/min) of form B; effect after heating to 50 °C.

heating form B. Both transitions are completely reversible and occur around 60–70 °C. These enantiotropic transitions are in agreement with the endothermic transitions found by DSC. Solvent mediated conversion experiments show that at room temperature polymorph B transforms to polymorph A, indicating that form A is thermodynamically more stable.

The reversibility with hardly any hysteresis is quite rare for organic crystals such as in this case. The reason for this (almost) completely reversible transition could be due to the same mechanism as

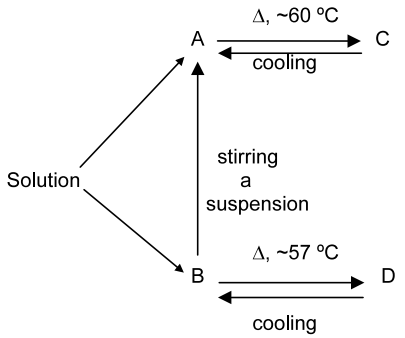

Fig. 15. Thermodynamic stability of different crystalline forms.

caused the disorder in the crystalline state of form B. Since the disorder is easily removed by annealing the sample at 50 °C, there must be a low energy barrier between the disordered and ordered state.

Finally, a schematic Gibbs free energy diagram Fig. 16, can be drawn. This shows that below approximately 70 °C polymorph A has the lowest Gibbs free energy and above 70 °C polymorph C has the lowest Gibbs free energy. The melting temperatures and enthalpies obtained by DSC (Tables 1 and 2) are associated with forms C and D. From these melting temperatures and melting enthalpies it seems that the forms C and D have a monotropic relation, that is form C is more stable (has an higher melting temperature and higher melting enthalpy) than form D. No conversion from form D to form C takes place during the applied measurement time.

4. Conclusions

Different analytical techniques, such as SS-NMR, XRPD, Raman spectroscopy and DSC, clearly show that Org 13011 exists as four polymorphs: two low temperature forms A and B and two high temperature forms C and D.

Upon heating, forms A and B do not transform into each other, but upon stirring a suspension of a mixture of both forms in ethanol form B transforms into form A. This shows that form A is the most stable form in the temperature range from

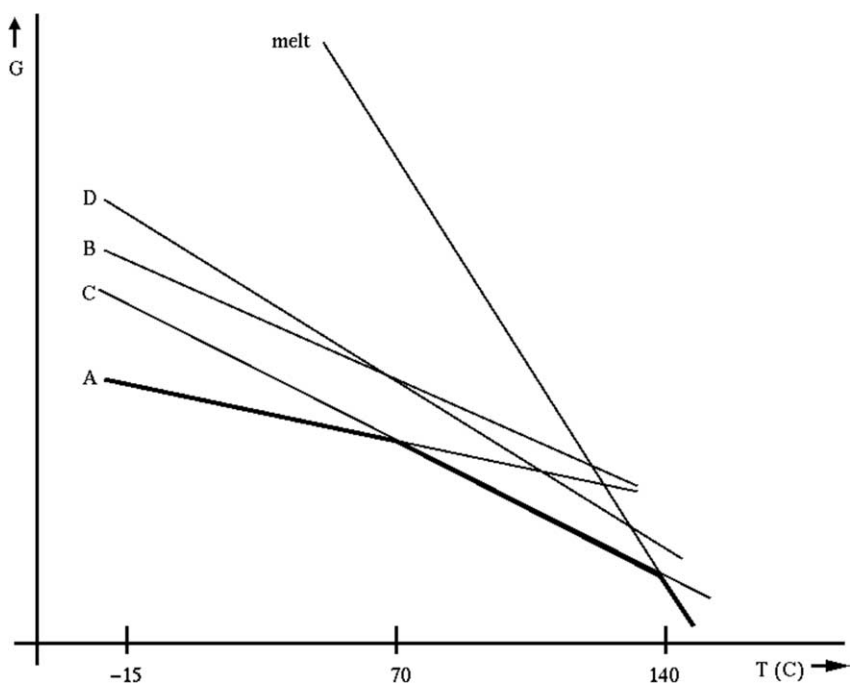

Fig. 16. Schematic free energy diagram of crystalline forms A, B, C and D.

room temperature to reflux temperature. It has been shown that forms A and C as well as forms B and D have an enantiotropic relation. Both transitions are reversible showing that only a small difference in crystal structure exists.

The broad endothermic peak of form B indicates a time dependent phenomenon (relaxation process) that is, according to the XRPD analysis, not related to a change in crystalline structure. This effect is not shown by form A.

Acknowledgements

We thank Dr F. Kaspersen of Organon, Oss for initiating the discussion on the polymorphism of Org 13011, Mr J.P.B. van Deursen of RGL, AkzoNobel Central Research for the high temperature SS-NMR experiments and Dr L. Fielding of Organon, Newhouse for carefully reading the manuscript.

References

Aguiar, A.J., Krc, J., Kinkel, A.W., Samyn, J.C., 1967. Effect of polymorphism on the absorption of chloramphenicol from chloramphenicol palmitate. J. Pharm. Sci. 56 (7), 847–853.

Bernstein, J., 1999. Disappearing and Reappearing Polymorphs, Lecture notes, 1st International Symposium on the Aspects of Polymorphism and Crystallization. Hinckley, Leicestershire, UK.

Brittain, H.G., 1997. Spectral methods for the characterization of polymorphs and solvates. J. Pharm. Sci. 86 (4), 405–412.

Burger, A., Ramberger, R., 1979. On the polymorphism of pharmaceuticals and other molecular crystals. I. Mikrochim. Acta [Wien] II, 259–271.

Chamot, E.M., Mason, C.W., 1938. Handbook of Chemical Microscopy, vol. I, second edition. Wiley, New York.

De Villiers, M.M., van der Watt, J.G., Lötter, A.P., 1991. The interconversion of the polymorphic forms of chloramphenicol palmitate (CAP) as a function of environmental temperature. Drug Dev. Ind. Pharm. 17 (10), 1295–1303.

De Villiers, M.M., van der Watt, J.G., Lötter, A.P., 1993. Kinetic study of the solid-state thermal interconversion of the polymorphic forms of chloramphenicol palmitate. Drug Dev. Ind. Pharm. 19 (14), 1731–1739.

Giron, D., 1995. Thermal analysis and calorimetric methods in the characterisation of polymorphs and solvates. Thermochim. Acta 248, 1–59.

Groth, P., 1877. Zeits. f. Krystall. Miner. Verlag von Wilhelm Engelmann, Leipzig.

Haleblian, J.K., 1975. Characterization of habits and crystalline modification of solids and their pharmaceutical applications. J. Pharm. Sci. 64 (8), 1269–1288.

Haleblian, J.K., McCrone, W., 1969. Pharmaceutical applications of polymorphism. J. Pharm. Sci. 58 (8), 911–929.

Kofler, L., Kofler, A., Brandstatter, M., 1954. Thermo Mikro-Methoden. Universitathverlag Wagner Ges. M.B.H, Insbruck.

Kuhnert-Brandstatter, M., Sollinger, H., 1990a. Thermal analytical and infrared spectroscopic investigations on polymorphic organic compounds VI. Mikrochim. Acta 3, 137–149.

Kuhnert-Brandstatter, M., Sollinger, H., 1990b. Thermal analytical and infrared spectroscopic investigations on polymorphic organic compounds VIII. Mikrochim. Acta 3, 247–258.

Mitra, A.K., Ghosh, L.K., Gupta, B.K., 1993. Development of methods for the preparation and evaluation of chloramphenicol palmitate ester and its biopharmaceutically effective metastable polymorphs. Drug Dev. Ind. Pharm. 19 (8), 971–980.

Mitscherlich, E., 1822. Annales de Chimie, 19, 350–419.

Mullins, J.D., Macek, T.J., 1959. Some pharmaceutical properties of Novobiocin. J. Am. Pharm. Assoc. 49 (4), 245–248.

Ostwald, W., 1897. Zeits. f Phys. Chem., 22, 306.

Reffner, J.A., Ferrillo, R.G., 1988. Thermal analysis of polymorphism. J. Therm. Anal. 34, 19–36.

Tawashi, R., 1969. Gastrointestinal absorption of two polymorphic forms of aspirin. J. Pharm. Pharmacol. 21, 701–702.

The Pharmaceutical Journal. 1998. Manufacturing problems hit Abbott's HIV drug ritonavir, p. 261.

Threfall, T.L., 1995. Analysis of organic polymorphs: a review. Analyst 120, 2435–2460.

Yu, L., 1995. Inferring thermodynamic stability relationship of polymorphs from melting data. J. Pharm. Sci. 84 (8), 966–974.